JOURNAL OF GEOPHYSICAL RESEARCH, VOL. 102, NO. B6, PAGES 12,085-12,094, JUNE 10, 1997

An improved algorithm for micromagnetics

T. M. Wright[1] and W. Williams

Department of Geology and Geophysics, University of Edinburgh, Edinburgh, Scotland

D. J. Dunlop

Department of Physics, University of Toronto, Toronto, Canada

Abstract. We present an improved micromagnetic model for predicting the minimum energy magnetization states in fine magnetite grains. The resolution, or the number of elemental magnetization vectors, has been increased over previous models: first, by the use of a Fourier transform algorithm to reduce the number of calculations from $\mathcal{O}(N^2)$ to $\mathcal{O}(N \log N)$ (N being the number of elements into which the grain is subdivided); and second, by implementing the model on a parallel computer. Using a parallel computer reduces the computation time by a factor of approximately $1/(4N_p)$, where N_p represents the number of processors. The improved model enables equilibrium magnetization states to be predicted using a resolution of $64 \times 64 \times 64$ subcubes to a grain in 16 hours of CPU time; this compares with a resolution of $12 \times 12 \times 12$ in 24 hours of CPU time for previous models. High-resolution models allow the examination of multidomain states in materials such as magnetite and different sized grains or assemblages of interacting grains.

Introduction

Recent developments in micromagnetic modeling have shown that magnetization states in magnetite grains above a critical size are nonuniform inhomogenous structures which require three-dimensional (3-D) models One of the important aspects of such models, which this study considers, is the resolution of the model or the number of elements which the grain is divided into. Micromagnetic models, such as the one shown in Figure 1a, model a cubic grain by dividing it into a number of elemental subcubes and assign a magnetic vector to the center of each subcube. Iterative minimization techniques are used to produce either a stable global-energy-minimum state or more generally a metastable local-energy-minimum (LEM) state. Previous models which have not used restrictive assumptions have been limited to using resolutions of not greater than $12 \times 12 \times 12$ [*Williams and Dunlop*, 1990], and higher-resolution results are required in order to confirm their predictions. In addition, higher-resolution models are required in order to determine the transition to conventional multidomain type states in larger grains. Attempts to increase the resolution have included using a two-dimensional model and truncating the interaction range [*Dunlop*, 1990], or imposing symmetry relations [*Williams and Dunlop*, 1989]. These models are likely to be inaccurate or to produce constrained solutions. This paper describes an improved micromagnetic algorithm which takes advantage of recent developments in parallel computing in order to predict new metastable domain states for magnetite (*T.M. Wright and W. Williams*, High-resolution micromagnetic analysis of pseudo-single-domain magnetic grains, submitted to *Journal of Geophysical Research*, 1996).

Recently, *Fabian et al.* [1996] independently developed a 3-D micromagnetic algorithm using a fast fourier transform (FFT) to produce a highly efficient code capable of relatively large resolutions of up to 33,327 interacting elements. However, their model assumes that the neighboring interacting elements must lie immediately adjacent and cannot be separated from each other. This essentially constrains their algorithm to modeling magnetic domain configurations of single grains. The method suggested here allows an arbitrary distance to separate neighboring elements and thus enables the behavior of magnetostatically interacting arrays of single-domain (SD) and pseudo-single-domain grains to be studied. Using parallel processing implemented on a Connection machine, a resolution of nearly 8 times (up to $64 \times 64 \times 64$ elements) that achieved by Fabian et al. can be obtained. In this way realistic geometries of interacting grains can be modeled and compared directly to recent experimental studies [*King et al.*, 1996].

The magnetization configuration in a real grain is assumed to occupy metastable equilibrium states, and ideally, these should be obtained in a manner which closely

[1]Now at Hewlett-Packard, Santa Rosa, California.

Paper number 96JB03628.
0148-0227/97/96JB-03628$09.00

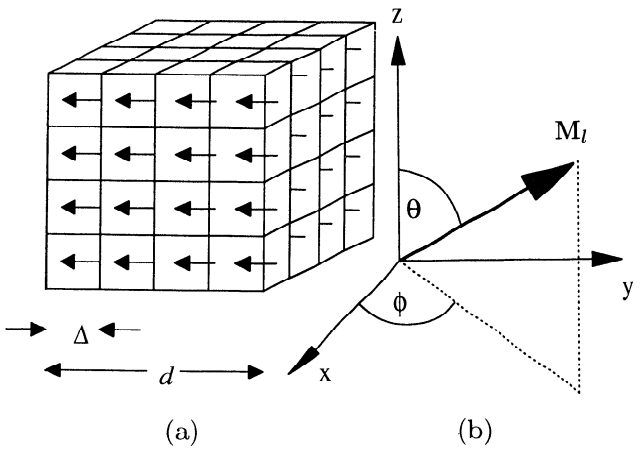

Figure 1. (a) A cubic crystal of edge length d is modelled by subdividing a cube into $N = n^3$ sub-cubes each of edge length Δ. In the above diagram $n = 4$. (b) Each elementary magnetization vector is defined by the azimuthal angle (ϕ) and the colatitudinal angle (θ).

resembles the physical process of the acquisition of a thermoremanent magnetization. That is, minimum energy states should be calculated by using a relaxation method stimulated by thermal fluctuations. Techniques such as simulated annealing attempt to mimic such processes and have proven very useful in a number of problems [*Kirkpartick et al.*, 1983]. Simulated annealing essentially consists of a random walk downhill, or occasionally uphill, if allowed by a probability based on a defined "temperature", equivalent to a thermal fluctuation. Simulated annealing methods have been used in micromagnetic calculation [*Thomson et al.*, 1994], but because of the random nature of the steps taken, the computational costs are very high. Because of the high computational requirements, the use of simulated annealing has been restricted to modeling low-resolution structures at small grain sizes.

The conjugate gradient (CG) method is a very powerful technique which is suited for large-scale minimization problems [*Powell*, 1977]. This is a first-order method, which for perfectly quadratic equations converges in $N(N+1)$ line minimizations, where N is the number of variables. Its advantages are that, although it does not require calculating and storing the Hessian, which may exceed the memory capacity of the computer, it still has a good convergence rate. The convergence rate is higher than simple steepest descent methods due to the use of a more sophisticated set of "noninterfering" search directions. If the storage of the Hessian is possible then a second-order method, such as a quasi-Newton (QN) method, should converge faster and have the advantage of avoiding false convergence due to inflection points in the objective function. However, as is often the case in large-scale problems, the Hessian can be so ill conditioned that the convergence rate is much slower than the CG method, even when damping of the Hessian is introduced. A comparison between CG and QN methods showed that, as expected, the extra CPU time required to compute the Hessian in the QN method was not compensated for by a sufficiently large increase in the convergence rate. The second-order method is still useful in confirming that true LEM states have been attained.

The magnetostatic energy calculation E^d is the most computationally expensive calculation as the interaction of each magnetization vector with every other vector needs to be considered. This makes the problem a so-called N body problem, requiring $\mathcal{O}(N^2)$ calculations, where N is the total number of cubic elements into which the grain is subdivided (Figure 1a). To model the magnetostatic energy interaction efficiently, ideally, each processor in a parallel computer would be connected to every other processor. However, in practice, parallel computers are normally constructed so that each processor is connected to only a few other processors. This means that E^d cannot be directly converted from a direct pairwise summation to a parallel, simultaneous sum, requiring $\mathcal{O}(N)$ calculations. N body problems are ubiquitous in science and a technique often used is a FFT method. This method increases the efficiency of the model: first, by reducing the number of calculations from $\mathcal{O}(N^2)$ to $\mathcal{O}(N \log N)$; and second, by enabling E^d to be implemented on a parallel computer.

This technique was first applied by *Giles et al.* [1990], who calculated E^d by using a two-dimensional FFT routine with periodic boundary conditions. A similar method was developed by *Yuan and Bertram* [1992] on low-resolution, two-dimensional magnetic systems with nonperiodic or nonmagnetic boundary conditions. Nonperiodic boundary conditions are important in modelling natural magnetic minerals with a finite size, and this paper describes an improved algorithm which increases the efficiency of the magnetostatic calculation by using a general 3-D FFT algorithm with nonperiodic boundary conditions. In addition, this paper describes how the accuracy of the exchange calculation can be improved by using a second-order expansion.

Description of Model

As the micromagnetic method has been described in detail by *Brown* [1978], only the extensions necessary for the three-dimensional formulation will be described. The essence of the micromagnetic approach is that it takes a semiclassical view of the physics of magnetism. That is, we do not want to describe the magnetization on the quantum mechanical level, but we need to describe it in sufficient detail to enable the magnetic structures to be accurately determined. The magnetization at any point within the material is averaged over many hundreds of unpaired electron spins and is taken to be a continuous function of position. The magnetization of each subcube is then modeled by a magnetic vector placed at its center and whose direction represents the direction of the average magnetization within that cubic element. The magnetization intensity of the subcube vectors is assumed to be constant and only their direction may alter in order to reduce the grain's to-

tal magnetic energy. The magnetic energy is evaluated in terms of the interactions between the magnetization vectors themselves and between the magnetization and the crystalline structure. Although the model described here has cubic elements, the methodology is completely general and valid for any cuboid subelement. Figure 1 shows the cubic system used. The edge length of the grain is denoted by d, and the cube is subdivided into $N = n^3$ subcubes, each of edge length Δ ($\Delta = d/n$). In the center of each subcube is an elementary magnetic vector $\mathbf{M}_l$ of constant magnitude M_s whose direction represents the average direction of all the atomic magnetic vectors within that subcube.

The magnetic energy is the sum of the magnetostatic E^d, the exchange E^e, the anisotropy E^a and the external field energies E^h. For each energy term, except for the exchange energy, the Cartesian coordinates of the subcube in the 3-D coordinate system will be abbreviated from ijk to the single subscript l. The direction of $\mathbf{M}_l$ varies with the azimuth ϕ and the colatitude θ and has direction cosines α, β, γ given by

$$\mathbf{m}_l = \frac{\mathbf{M}_l}{M_s} = \begin{pmatrix} \alpha_l \\ \beta_l \\ \gamma_l \end{pmatrix} = \begin{pmatrix} \cos(\phi_l)\sin(\theta_l) \\ \sin(\phi_l)\sin(\theta_l) \\ \cos(\theta_l) \end{pmatrix}. \quad (1)$$

The algorithm was implemented on a 16000 processor, TMC Connection Machine CM-200 data parallel computer which associates a few data elements with each processor [*Hillis*, 1985]. In the specific example of micromagnetism, each data element corresponds to the azimuthal and colatitude of each elementary vector, as shown in Figure 1.

Discretization of the Energy Terms

For each energy term, integration over the volume of the grain is approximated by a sum over the subcubes in which a continuous function $f(\theta, \phi)$ is replaced by a discrete function f_l,

$$E^e = \int\int\int f(\theta,\phi)dx\,dy\,dz \approx \sum_l f_l \tau, \quad (2)$$

where $\tau = \Delta^3$ is the volume of each subcube and the sum is over each of the three dimensions.

Exchange Energy

Using the approximation that the angle between atomic spins is small, *Brown* [1978] obtained the following expression for the exchange energy E^e,

$$E^e = \frac{C_e}{2}\int(\nabla\mathbf{m})^2 dV = \frac{C_e}{2}\sum_{i,j,k}(\nabla\mathbf{m}_{ijk})^2\Delta^3. \quad (3)$$

A first-order approximation would be to assume that the magnetization varies linearly between subcubes. Using $\mathbf{m}\cdot\mathbf{m} = 1$, and considering the i direction,

$$\begin{aligned}(\nabla\mathbf{m}_{ijk})^2 &= \frac{(\mathbf{m}_{(i+1)jk} - \mathbf{m}_{ijk})^2}{\Delta^2} \\ (\nabla\mathbf{m}_{ijk})^2 &= \frac{2}{\Delta^2}(1 - \mathbf{m}_{ijk}\cdot\mathbf{m}_{(i+1)jk}) \quad (4)\end{aligned}$$

giving

$$E^e = \Delta C_e \sum_{i=1}^{n-1}\sum_{j=1}^{n-1}\sum_{k=1}^{n-1}(1 - \mathbf{m}_{ijk}\cdot\mathbf{m}_{(i+1)jk}), \quad (5)$$

plus similar expressions for the j and k directions. A more accurate approximation would be to start from equation (3) and use Green's formula,

$$\begin{aligned}E^e &= \frac{C_e}{2}\int(\nabla\mathbf{m})^2 dV \\ E^e &= -\frac{C_e}{2}\left(\int \mathbf{m}\cdot\nabla^2\mathbf{m}dV + \int\nabla\mathbf{m}\frac{\partial\nabla\mathbf{m}}{\partial n}dS\right) \\ E^e &= -\frac{C_e}{2}\Delta^3\sum_{i,j,k}\mathbf{m}_{ijk}\cdot\nabla^2\mathbf{m}_{ijk} \quad (6)\end{aligned}$$

where the second term vanishes due to the boundary condition $\partial\mathbf{m}/\partial n = 0$ at the grain surface.

A five point difference scheme in one dimension is given by

$$\frac{\partial^2 f}{\partial x^2} = \frac{1}{12}\frac{-f_{i-2} + 16f_{i-1} - 30f_i + 16f_{i+1} - f_{i+2}}{\Delta^2}, \quad (7)$$

so in three dimensions, equation (6) becomes

$$E^e = -\frac{C_e\Delta^3}{2}\sum_{i=1}^{n}\sum_{j=1}^{n}\sum_{k=1}^{n}\mathbf{m}_{ijk}\cdot\nabla^2\mathbf{m}_{ijk}, \quad (8)$$

where ∇^2 is the five point difference (equation (7)) extended to three dimensions.

To ensure that the boundary condition, $\partial\mathbf{m}/\partial n = 0$, is satisfied (in this case n is the outward normal to the grain boundary) the magnetization needs to be re-

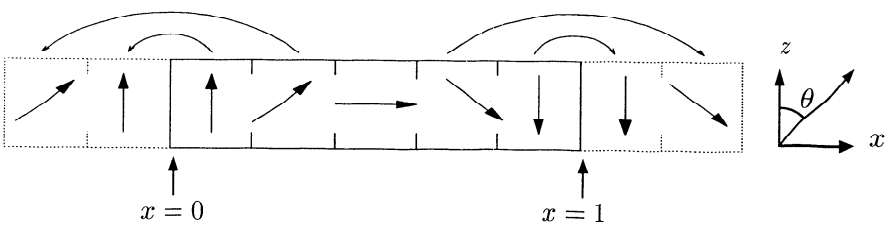

Figure 2. A one-dimensional system with $n = 5$ showing how the boundary conditions are satisfied for the five point exchange formulation. A similar scheme is used for the linear exchange formulation but only the sub-cube nearest the boundary is reflected.

flected at the boundary. Figure 2 shows that for a one-dimensional (1-D) system using the five-point exchange formulation the vectors need to be copied from the two subcubes nearest the surface. This is purely a mathematical device and does not imply that any type of periodic boundary conditions have been imposed.

The two formulations were compared using the arbitrary array of magnetization vectors shown in the 1-D domain wall of Figure 2. The vectors are described by the colatitude θ, which varies with the distance x, and the azimuthal angle ϕ which is kept equal to zero. The spins on the outer edges are approximately $\pi/2$ radians apart and the intermediate spins are described by a balance between an exchange energy term and a uniaxial anisotropy energy [*Chikazumi and Charap*, 1964].

$$\theta = 2\tan^{-1}(10^x) \tag{9}$$

Figure 3 shows how the exchange energy depends on the resolution. Both formulations converge to the same value, but the five-point formulation converges at a lower resolution and is thus more accurate. Figure 4 shows how the exchange energy depends on the angle between two spins (i.e., Figure 2 with a resolution of $n = 2$). The spin at $x = 0$ is kept fixed, and the neighboring spin varied from $\theta = 0°$ to $\theta = 360°$. The need to reflect both boundaries to a depth of two subcubes allows the five-point exchange formulation to be compared with the linear exchange at a resolution of $n = 2$. The five-point formulation results in higher values of E^e for all angles of θ. Although the same value of the exchange constant was used for both formulations, the five-point formulation effectively produces a stiffer exchange interaction between the spins. This means that the five-point formulation is less likely to produce magnetization states in which neighboring spins have large angles between them. Thus although the five-point exchange formulation is in general more accurate than the liner approximation, it is important to realize that significant errors may still be present. For example, vortex domain structures may be more difficult to nucleate since neighboring spins near the vortex center are separated by large angles and a stiffer exchange may penalize this. The CPU time required to calculate the exchange energy is much less than that required for the demagnetizing energy, so the choice of exchange formulation has no significant impact on the efficiency of the micromagnetic algorithm.

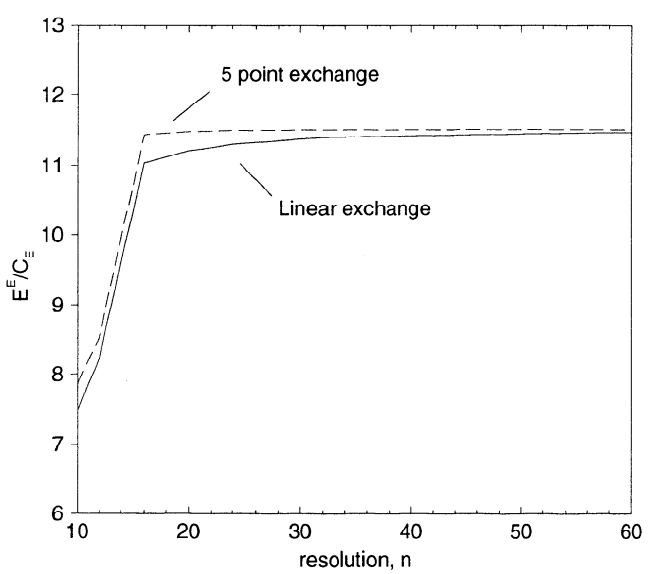

Figure 3. Dependence of the exchange energy (E^e) on the resolution n, solid curve, linear formulation; dashed curve, five point formulation.

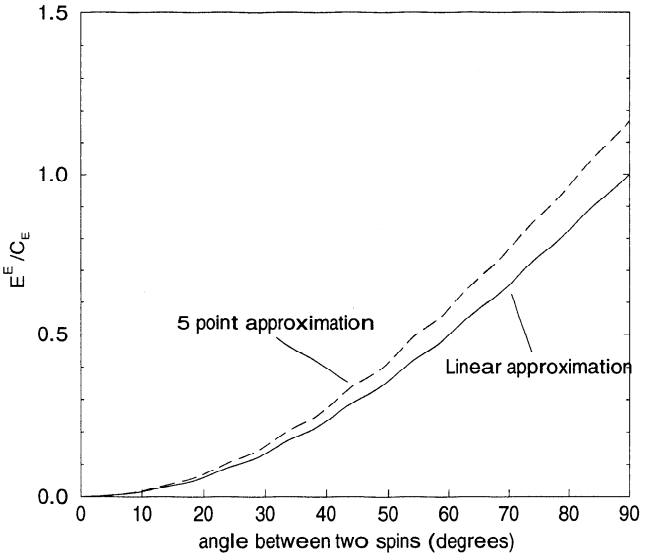

Figure 4. Dependence of the exchange energy (E^e) on the angle θ between two spins: solid curve, linear formulation; dashed curve, five point formulation.

Anisotropy Energy

The cubic anisotropy is approximated by using the first anisotropy constant K_1 and is a local term independent of the resolution.

$$E^a = \frac{K_1}{2}\sum_l (1 - (\mathbf{m}_l)^4)\Delta^3. \tag{10}$$

For magnetite and nickel, K_1 is negative. The easy $\langle 111 \rangle$ and intermediate $\langle 110 \rangle$ directions are low-energy directions, whereas the hard $\langle 100 \rangle$ directions are high energy directions. The convention used in this study will be that $E^a = 0$ for a SD state aligned along one of the $\langle 100 \rangle$ hard directions, and $E^a < 0$ for a SD state aligned in one of the $\langle 111 \rangle$ or $\langle 110 \rangle$ easy directions.

External Field Energy

Applying an external field $\mathbf{H}$ to the model with magnitude H and direction θ_H and ϕ_H gives as an expression for E^h,

$$E^h = -\mu_0 \sum_l M_s \mathbf{H} \cdot \mathbf{m}_l \Delta^3. \tag{11}$$

Magnetostatic Energy

This section describes how the FFT technique can be extended to calculate the magnetostatic energy for three-dimensional systems. Using Maxwell's equations for the field $\mathbf{H}'$ due to each elementary magnetic vector,

$$\nabla \times \mathbf{H}' = \frac{4\pi}{c}\mathbf{J}, \tag{12}$$

and assuming that the current density $\mathbf{J}$ equals zero, we can define a scalar potential Φ such that $\mathbf{H}' = -\nabla\Phi$.

For a ferromagnet with volume V_2 and surface S_2, the potential at a point $\mathbf{r}_1$ due to a magnetostatic charge at $\mathbf{r}_2$ can be calculated using Green's functions [*Jackson*, 1975]

$$\Phi(\mathbf{r}_1) = -\frac{1}{4\pi}\int_V \frac{\nabla\cdot\mathbf{M}(\mathbf{r}_2)}{|\mathbf{r}_1-\mathbf{r}_2|}dV_2 + \frac{1}{4\pi}\oint_S \frac{\mathbf{M}(\mathbf{r}_2)\cdot\mathbf{n}_2}{|\mathbf{r}_1-\mathbf{r}_2|}dS_2. \tag{13}$$

The model described in this study assumes that the magnetization within each subcube is of constant direction and magnitude ($\nabla\cdot\mathbf{M}=0$). Equation (13) then reduces to solely the second term, and the calculation becomes a sum over charged plates. Two methods for splitting a cubic system into charged plates have previously been used: (1) *Berkov et al.* [1993] used an algorithm in which the fundamental unit is a charged plate and the calculation is a sum over each charged plate. In this case the charge on each plate is a function of the difference in the magnetization directions in the neighboring subcubes, so that the subcubes cannot be separated; and (2) *Williams and Dunlop* [1989] considered the fundamental unit to be a pair of charged subcubes and the calculation to be a sum over each subcube. Both schemes were implemented using a conventional N^2 serial algorithm and were found to be identical in terms of the accuracy and the number of calculations required (the difference in E^d between the two schemes was less than $10^{-7}\%$). However, using the subcube as the fundamental unit means that it is easy to modify the distance between subcubes from zero to some arbitrary distance. This therefore provides a more flexible algorithm and allows the investigation of grain interactions, where each subcube represents a complete SD grain, or group of subcubes can represent a simple pseudo-single-domain grain. In addition, by varying the dimension of the model from three dimensional to two dimensional, interactions between SD grains either as in thin films or a 3-D assemblage could be studied.

By using the divergence theorem, $\int_V \nabla\cdot\mathbf{F}dV = \int_S \mathbf{F}\cdot\mathbf{n}dS$, and denoting σ_l as the charge density on plate l, ($\sigma = \mathbf{m}\cdot\mathbf{n}$, $\sigma\in\{\alpha,\beta,\gamma\}$), the energy per unit volume between the two plates shown in Figure 5 becomes

$$\begin{aligned} E^d_{lm} &= -\mu_0\int \mathbf{M}(\mathbf{r}_l)\cdot\mathbf{H}'dV = \mu_0\int \mathbf{M}(\mathbf{r}_l)\cdot\nabla\Phi dV \\ E^d_{lm} &= \mu_0\int[\nabla\cdot(\Phi\mathbf{M}(\mathbf{r}_l)) - \Phi\nabla\cdot\mathbf{M}(\mathbf{r}_l)]\,dV \\ E^d_{lm} &= \mu_0 M_s\int_{S_l}\sigma_l\Phi dS_l. \end{aligned} \tag{14}$$

The potential Φ at l due to the plate at position m is given by the second term in (13), so E^d_{lm} becomes

$$\begin{aligned} E^d_{lm} &= \frac{\mu_0 M_s^2}{4\pi}\int_{S_l}\int_{S_m}\frac{\sigma_l\sigma_m}{|\mathbf{r}_l-\mathbf{r}_m|}dS_l dS_m \\ E^d_{lm} &= \frac{\mu_0 M_s^2}{4\pi}W_{l-m}\sigma_m\sigma_l, \end{aligned} \tag{15}$$

where W_{l-m} is calculated using the method of *Rhodes and Rowlands* [1954]. For example, for the two orthogonal plates shown in Figure 5, with (y_l, z_l) and (x_m, z_m) the set of points inside the charged plates σ_l and σ_m respectively, then W_{l-m} is given by

$$W_{l-m} = \int_0^\Delta\int_0^\Delta\int_0^\Delta\int_0^\Delta \frac{1}{r}dy_l dz_l dx_m dz_m, \tag{16}$$

where r is the distance between (y_l, z_l) and (x_m, z_m). W_{l-m} forms a demagnetizing tensor similar to that reported by *Newell et al.* [1993]. The appendix describes the evaluation of the integral in (16). Figure 6 shows the four interactions which make up $W^{\alpha\beta}$. The energy between the α plates at cube l and the β plates at cube m for the whole system is given by

$$E^d = \frac{\mu_0 M_s^2}{8\pi}\sum_l\sum_m W^{\alpha\beta}_{l-m}\alpha_l\beta_m. \tag{17}$$

where α_l and β_m are the charge densities (σ) on the plates. All summations are assumed to be from 1 to n

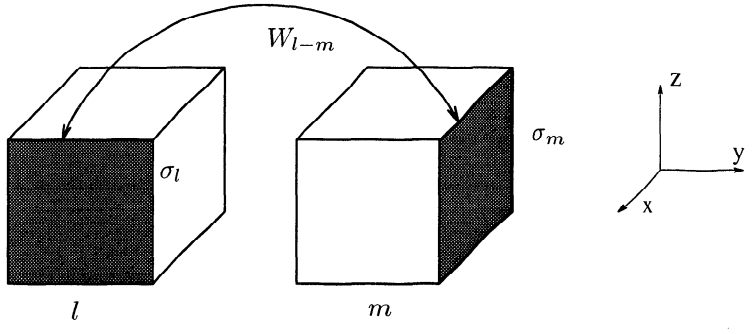

Figure 5. Magnetostatic interaction between two orthogonal plates.

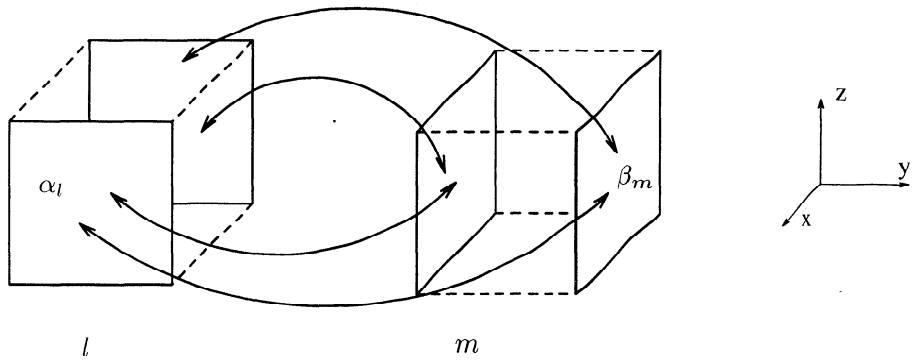

Figure 6. The four interactions required for each configuration of charged plates. $W^{\alpha\beta}$ is the sum of each of the four interactions shown.

in each of the three dimensions. A factor of a half has been introduced in order to cancel the effect of counting combinations of plates twice during the full double summation. The total energy is the sum of each interaction between α, β, and γ plates including the self energy of each subcube.

Fast Fourier Transform Method

Equation (17) requires $\mathcal{O}(N^2)$ calculations but by rewriting in terms of a convolution and calculating in frequency space, the number of calculations can be reduced to $\mathcal{O}(N \log N)$. Absolute time savings made using the FFT method compared with the normal N^2 calculation will be dependent on the CPU type and FFT algorithm. However, since the FFT method incurs a significant extra bookkeeping overhead, overall CPU time savings will not be made for models of resolutions less than $7 \times 7 \times 7$.

The energy between the surface charges σ_l and σ_m is given by

$$E^d = \frac{\mu_0 M_s^2}{8\pi} \sum_l \sum_m W_{l-m} \sigma_l \sigma_m. \tag{18}$$

Using $\tilde{\sigma}$ to represent the discrete Fourier transform coefficients of σ,$\sigma \Longleftrightarrow \tilde{\sigma}$,

$$\sigma_l = \frac{1}{N} \sum_k \tilde{\sigma}_k \exp[-2\pi i k l/N] \tag{19}$$

$$\sigma_m = \frac{1}{N} \sum_{k'} \tilde{\sigma}_{k'} \exp[-2\pi i k' m/N] \tag{20}$$

$$W_{l-m} = \frac{1}{N} \sum_{k''} \tilde{W}_{k''} \exp[-2\pi i k''(l-m)/N]. \tag{21}$$

Equation (18) now becomes

$$E^d = \frac{\mu_0}{8\pi N^3} \sum_l \sum_m \sum_k \sum_{k'} \sum_{k''} \tilde{\sigma}_k \tilde{\sigma}_{k'} \tilde{W}_{k''} \cdot \exp[-2\pi i[l(k+k'') + m(k'-k'')]/N] \tag{22}$$

and using the definition of a delta function,

$$\delta(k+k'') = N \sum_{l=1}^{N} e^{-2\pi i(k+k'')l/N} = \begin{cases} 1 & k+k''=0 \\ 0 & k+k'' \neq 0 \end{cases} \tag{23}$$

$$E^d = \frac{\mu_0}{8\pi N} \sum_k \sum_{k'} \sum_{k''} \tilde{\sigma}_k \tilde{\sigma}_{k'} \tilde{W}_{k''} \delta(k+k'') \delta(k'-k''). \tag{24}$$

The first delta function has a value of 1 only when $k'' = -k$ and the second when $k' = k'' = -k$. Therefore

$$E^d = \frac{\mu_0}{8\pi N} \sum_k \tilde{\sigma}_k \tilde{\sigma}_{-k} \tilde{W}_{-k}, \tag{25}$$

and as the array W is an even function, then $\tilde{W}$ is real and it follows that $W_k = W_{-k}$, giving

$$E^d = \frac{\mu_0}{8\pi N} \sum_k \tilde{\sigma}_k \tilde{\sigma}_{-k} \tilde{W}_k. \tag{26}$$

The expression for the complete magnetostatic energy calculated in frequency space is given by

$$E^d = \frac{\mu_0 M_s^2}{4\pi N} \sum_k (\tilde{\mathbf{m}}_k \tilde{\mathbf{W}}_k) \cdot \tilde{\mathbf{m}}_{-k}, \tag{27}$$

where $\tilde{\mathbf{W}}_k$ is the tensor

$$\tilde{\mathbf{W}}_k = \begin{bmatrix} \frac{1}{2}\tilde{W}^{\alpha\alpha} & \frac{1}{2}\tilde{W}^{\alpha\beta} & \frac{1}{2}\tilde{W}^{\alpha\gamma} \\ \frac{1}{2}\tilde{W}^{\beta\alpha} & \frac{1}{2}\tilde{W}^{\beta\beta} & \frac{1}{2}\tilde{W}^{\beta\gamma} \\ \frac{1}{2}\tilde{W}^{\gamma\alpha} & \frac{1}{2}\tilde{W}^{\gamma\beta} & \frac{1}{2}\tilde{W}^{\gamma\gamma} \end{bmatrix}. \tag{28}$$

As $W^{\alpha\beta} = W^{\beta\alpha}$ and $\tilde{W}$ is real, the number of calculations can be reduced by writing

$$\frac{1}{2} \sum_k \tilde{\alpha}_k \tilde{\beta}_{-k} \tilde{W}^{\alpha\beta} + \frac{1}{2} \sum_k \tilde{\beta}_k \tilde{\alpha}_{-k} \tilde{W}^{\beta\alpha} = \sum_k \tilde{\alpha}_k \tilde{\beta}_{-k} \tilde{W}^{\alpha\beta}, \tag{29}$$

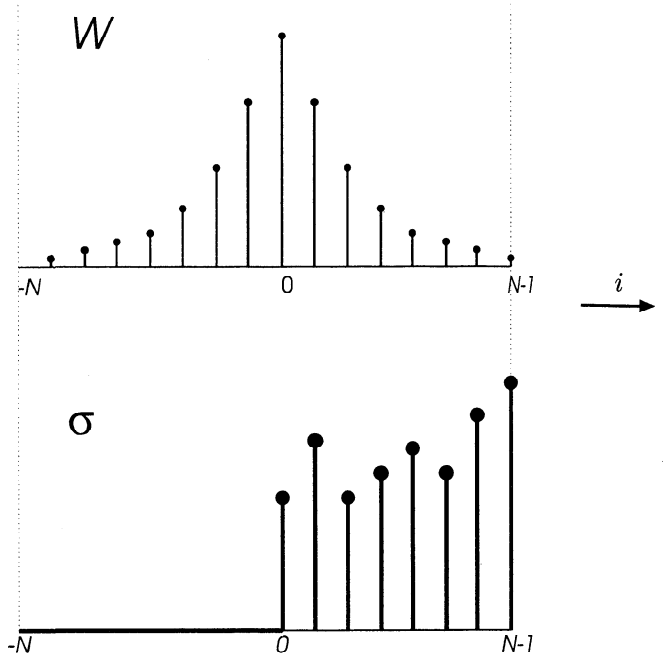

Figure 7. Arrangement of the interaction coefficients (W) and the array of charges (σ) for a one-dimensional model with $N = 8$. In this example W is an even function, W at $i = 0$ represents the self-energy of the subcube, W at $i = -N$ is equal to zero.

and the modified tensor $\mathbf{W}_k$ now becomes

$$\tilde{\mathbf{W}}_k = \begin{bmatrix} \frac{1}{2}\tilde{W}^{\alpha\alpha} & \tilde{W}^{\alpha\beta} & \tilde{W}^{\alpha\gamma} \\ 0 & \frac{1}{2}\tilde{W}^{\beta\beta} & \tilde{W}^{\beta\gamma} \\ 0 & 0 & \frac{1}{2}\tilde{W}^{\gamma\gamma} \end{bmatrix} . \quad (30)$$

Implementing Nonperiodic Boundaries

The convolution theorem assumes that the surface charges (σ) are periodic in each of the three directions whereas real magnetite grains have a finite size with non-magnetic or free-air boundaries. Figure 7 shows how the interaction array W and the charges (σ) have to be arranged for a one dimensional system with $N = 8$ in order to satisfy nonperiodic boundary conditions. For both W and σ, arrays have to be allocated in which each dimension is twice as large as the resolution of the model. For example, a 3-D model with a resolution of $32 \times 32 \times 32$ subcubes requires arrays of size $64 \times 64 \times 64$ to be allocated. The additional values of the charges σ are set to zero in order to model free-air boundary conditions [*Press et al.*, 1986]. The additional values of the array W between $i = -1$ and $i = -N$ represent the interaction when the subcube m (shown in Figure 5) is to the left of subcube l. A similar method is implemented in the two other dimensions for the 3-D model.

Conclusion

By using fast Fourier transforms to calculate the magnetostatic energy, we have developed the most efficient micromagnetic algorithm to date, and using individual subcubes as the discrete element results in the most general algorithm. In addition to modeling cubic grains, a high-resolution cubic system is a general model which can be used as a starting point from which to model arbitrarily shaped grains. With high resolutions, up to $64 \times 64 \times 64$, the computation time on a parallel computer is sufficiently fast to allow metastable equilibrium states to be calculated using iterative optimization techniques. At lower resolutions, the computation time is reduced sufficiently, compared to previous algorithms, to make the use of the FFT algorithm worthwhile.

For example, using a resolution of $32 \times 32 \times 32$, a single energy calculation on the Connection Machine CM-200 takes 0.68 s, which compares to 32,768 s on a Stardent GS1000 serial machine. Taking into account the fact that the GS1000 is a four-processor vector machine and the CM-200 a $N_p = 16,000$ processor parallel machine, the computation time for the CM-200 model is faster by approximately $1/(4N_p)$.

Appendix: Interaction Coefficients

Much computer time can be saved by resolving each dipole into its equivalent magnetostatic surface charges and evaluating the interaction between these charged sheets in the manner of *Rhodes and Rowlands* [1954]. In this way the angular and spatial components of the interactions can be separated and the invariant spatial components evaluated once and stored in a look-up table. The angular component simply represents the varying magnetostatic charges on the surface as the direction of each elementary vector changes.

If we represent the magnetostatic charges on a pair of interacting sheets in the xy plane as σ_1 and σ_2, then the interaction energy E_m is given by

$$E_m = \sigma_2 \int_0^{\Delta} \int_0^{\Delta} V(x_2, y_2, z_2) dx_2 dy_2, \quad (31)$$

where $V(x_2, y_2, z_2)$ is the magnetic potential at the point (x_2, y_2, z_2) on the second sheet, due to the magnetic charge of the first. Thus

$$V(x_2, y_2, z_2) = \sigma_1 \int_0^{\Delta} dx_1 \int_0^{\Delta} \left((x_2 - x_1)^2 + (y_2 - y_1)^2 + z_2^2\right)^{-1/2} dy_1, \quad (32)$$

where Δ is the edge length of the sheets.

For one-dimensional models, only interactions between parallel sheets need be evaluated; however, for three-dimensional models, both parallel and orthogonal interactions must be calculated. Care must be taken when evaluating the integral to ensure that the limits are of the same sign. The case of interacting parallel sheets has been described by *Rhodes and Rowlands* [1954] and can be described in terms of a function $\mathcal{F}(x, y, z)$.

$$
\begin{aligned}
2\mathcal{F}(x,y,z) &= z^2x\,\sinh^{-1}\left(\frac{x}{y^2+z^2}\right)+y^2z\,\sinh(z/y)\\
&+x^2z\,\sinh^{-1}\left(\frac{z}{x^2+y^2}\right)\\
&+y^2x\,\sinh^{-1}(x/y)\\
&+xyz\,\tan^{-1}\left(\frac{(x^2+y^2+z^2)^{1/2}y}{xz}\right)\\
&+\frac{2}{3}y^2(x^2+y^2+z^2)^{-1/2}\\
&+\frac{1}{3}x^2(x^2+y^2)^{-1/2}-\frac{2}{3}y^2(x^2+y^2)^{1/2}\\
&+\frac{1}{3}z^2(y^2+z^2)^{-1/2}-\frac{2}{3}y^2(y^2+z^2)^{1/2}\\
&-y^2x\,\sinh^{-1}\left(\frac{x}{y^2+z^2}\right)+\frac{2}{3}y^3\\
&-y^2z\,\sinh^{-1}\left(\frac{z}{x^2+y^2}\right)-\pi xyz\\
&-\frac{1}{3}(x^2+z^2)(x^2+y^2+z^2)^{-1/2} \qquad (33)
\end{aligned}
$$

for interaction between pairs of $x-y$ planes. For interacting orthogonal planes the integral to be evaluated is similar to (32) except that for an xy plane interacting with an xz plane the integration in (31) is now over x and z. The result can be represented in terms of a function $\mathcal{G}(x,y,z)$:

$$
\begin{aligned}
\mathcal{G}(x,y,z) &= xyz+\ln(r+x)+\frac{1}{2}x^2y\,\ln(r+z)\\
&+\frac{1}{2}x^2z\,\ln(r+y)+\frac{1}{12}y^3\,\ln(x^2+y^2)\\
&+\frac{1}{12}z^3\,\ln(x^2+z^2)-\frac{1}{6}z^3\,\ln(r+y)\\
&+\frac{1}{6}z^3\,\ln\left((z^2+y^2)^{1/2}+y\right)-\frac{1}{6}y^3\,\ln(y)\\
&+\frac{1}{6}y^3\,\ln\left((z^2+y^2)^{1/2}+z\right)-\frac{1}{3}rzy\\
&+\frac{1}{6}x^3\,\tan^{-1}\left(\frac{rx}{yz}\right)+\frac{1}{2}y^2x\,\tan^{-1}\left(\frac{ry}{xz}\right)\\
&+\frac{1}{2}z^2x\,\tan^{-1}\left(\frac{rz}{xy}\right)+\frac{1}{3}zy(y^2+z^2)^{1/2}\\
&-\frac{1}{2}xyz\,\ln(y^2+z^2)-\frac{1}{6}y^3\,\ln(r+z)\\
&-\frac{1}{4}x^2y\,\ln(x^2+y^2)-\frac{1}{4}x^2z\,\ln(x^2+z^2)\\
&-\frac{1}{6}z^3\,\ln(z)-\frac{1}{4}\pi x(x^2+3y^2+3z^2) \qquad (34)
\end{aligned}
$$

where $r=(x^2+y^2+z^2)^{1/2}$. The functions needed for interactions between other pairs of orthogonal sheets can be obtained by symmetry.

The convolution theorem requires the interaction between the subcube at position $i=1$, $j=1$, $k=1$ and each of the other subcubes. The interaction coefficients, in terms of the function $\mathcal{G}$, between the subcube at coordinates $(i=1,j=1,k=1)$ and a subcube at coordinates $i\Delta=a$, $j\Delta=b$, $k\Delta=c$ is given by

$$
\begin{aligned}
W^{\beta\gamma} &= 2[\mathcal{G}(\Delta+a,b,2\Delta+c)+\mathcal{G}(\Delta+a,b,c)\\
&+\mathcal{G}(a,b,\Delta+c)+\mathcal{G}(2\Delta+a,b,\Delta+c)\\
&+4\mathcal{G}(\Delta+a,\Delta+b,\Delta+c)\\
&+\mathcal{G}(a,\Delta+b,2\Delta+c)+\mathcal{G}(a,\Delta+b,c)\\
&+\mathcal{G}(2\Delta+a,\Delta+b,2\Delta+c)\\
&+\mathcal{G}(2\Delta+a,\Delta+b,c)\\
&+\mathcal{G}(\Delta+a,2\Delta+b,2\Delta+c)\\
&+\mathcal{G}(\Delta+a,2\Delta+b,c)+\mathcal{G}(a,2\Delta+b,\Delta+c)\\
&+\mathcal{G}(2\Delta+a,2\Delta+b,\Delta+c)]\\
&-4\mathcal{G}(\Delta+a,b,\Delta+c)+\mathcal{G}(a,b,2\Delta+c)\\
&+\mathcal{G}(a,b,c)+\mathcal{G}(2\Delta+a,b,2\Delta+c)\\
&+\mathcal{G}(2\Delta+a,b,c)\\
&+4[\mathcal{G}(\Delta+a,\Delta+b,2\Delta+c)\\
&+\mathcal{G}(\Delta+a,\Delta+b,c)+\mathcal{G}(a,\Delta+b,\Delta+c)\\
&+\mathcal{G}(2\Delta+a,\Delta+b,\Delta+c)\\
&+\mathcal{G}(\Delta+a,2\Delta+b,\Delta+c)]\\
&+\mathcal{G}(a,2\Delta+b,2\Delta+c)+\mathcal{G}(a,2\Delta+b,c)\\
&+\mathcal{G}(2\Delta+a,2\Delta+b,2\Delta+c)\\
&+\mathcal{G}(2\Delta+a,2\Delta+b,c) \qquad (35)
\end{aligned}
$$

where a, b and c are in units of Δ. From symmetry,

$$W^{\alpha\gamma}(\alpha,\beta,\gamma)=W^{\beta\gamma}(\beta,\alpha,\gamma) \qquad (36)$$

Rhodes and Rowlands [1954]

$$W^{\alpha\beta}(\alpha,\beta,\gamma)=W^{\beta\gamma}(\gamma,\beta,\alpha). \qquad (37)$$

The coefficient $W^{\beta\beta}$ is given by

$$
\begin{aligned}
W_4^{\beta\beta} &= 2[(\mathcal{F}(2\Delta+a,\Delta+b,2\Delta+c)\\
&+\mathcal{F}(2\Delta+a,\Delta+b,c)\\
&+4\mathcal{F}(\Delta+a,\Delta+b,\Delta+c)\\
&+\mathcal{F}(a,\Delta+b,2\Delta+c)+\mathcal{F}(a,\Delta+b,c)\\
&+\mathcal{F}(2\Delta+a,b,\Delta+c)\\
&+\mathcal{F}(\Delta+a,b,2\Delta+c)\\
&+\mathcal{F}(\Delta+a,b,c)+\mathcal{F}(a,b,\Delta+c)\\
&+\mathcal{F}(2\Delta+a,2\Delta+b,\Delta+c)\\
&+\mathcal{F}(\Delta+a,2\Delta+b,2\Delta+c)\\
&+\mathcal{F}(\Delta+a,2\Delta+b,c)\\
&+\mathcal{F}(a,2\Delta+b,\Delta+c)]\\
&-4[\mathcal{F}(2\Delta+a,\Delta+b,\Delta+c)\\
&+\mathcal{F}(\Delta+a,\Delta+b,2\Delta+c)\\
&+\mathcal{F}(\Delta+a,\Delta+b,c)+\mathcal{F}(a,\Delta+b,\Delta+c)]\\
&-\mathcal{F}(2\Delta+a,b,2\Delta+c)-\mathcal{F}(2\Delta+a,b,c)\\
&-4\mathcal{F}(\Delta+a,b,\Delta+c)+\mathcal{F}(a,b,2\Delta+c)\\
&-\mathcal{F}(a,b,c)-\mathcal{F}(2\Delta+a,2\Delta+b,2\Delta+c)\\
&+\mathcal{F}(2\Delta+a,2\Delta+b,c)\\
&-4\mathcal{F}(\Delta+a,2\Delta+b,\Delta+c)\\
&+\mathcal{F}(a,2\Delta+b,2\Delta+c)\\
&+\mathcal{F}(a,2\Delta+b,c) \qquad (38)
\end{aligned}
$$

Because the limits of integration of (31) and (32) have to be split differently depending on the relative positions of the interacting sheets, the following conditions have to be taken into consideration:

1. When $i' \neq 1, j' \neq 1, k' = 1$, $W^{\alpha\beta} = W^{\beta\gamma} = 0$, $W^{\alpha\gamma} = W^{*\alpha\gamma}$ and $W^{\alpha\alpha} = W_3^{\alpha\alpha}$, $W^{\beta\beta} = W_{5a}^{\beta\beta}$, $W^{\gamma\gamma} = W_{5a}^{\gamma\gamma}$.
2. When $i' = 1, j' \neq 1, k' \neq 1$, $W^{\alpha\beta} = W^{*\alpha\beta}$, $W^{\beta\gamma} = W^{\alpha\gamma} = 0$ and $W^{\alpha\alpha} = W_{5b}^{\alpha\alpha}$, $W^{\beta\beta} = W_{5b}^{\beta\beta}$, $W^{\gamma\gamma} = W_3^{\gamma\gamma}$.
3. When $i' \neq 1, j = 1, k \neq 1$, $W^{\alpha\beta} = W^{\alpha}\gamma = 0$, $W^{\beta\gamma} = W^{*\beta\gamma}$ and $W^{\alpha\alpha} = W_{5c}^{\alpha\alpha}$, $W^{\beta\beta} = W_3^{\beta\beta}$, $W^{\gamma\gamma} = W_{5c}^{\gamma\gamma}$.
4. When $i' \neq 1, j' = 1, k' = 1$, $W^{\alpha\beta} = W^{\beta\gamma} = W^{\alpha\gamma} = 0$ and $W^{\alpha\alpha} = W_{2a}^{\alpha\alpha}$, $W^{\beta\beta} = W_{2a}^{\beta\beta}$, $W^{\gamma\gamma} = W_1^{\gamma\gamma}$.
5. When $i' = 1, j' = 1, k' \neq 1$, $W^{\alpha\beta} = W^{\beta\gamma} = W^{\alpha\gamma} = 0$ and $W^{\alpha\alpha} = W_1^{\alpha\alpha}$, $W^{\beta\beta} = W_{2b}^{\beta\beta}$, $W^{\gamma\gamma} = W_{2b}^{\gamma\gamma}$.
6. When $i' = 1, j' \neq 1, k' = 1$, $W^{\alpha\beta} = W^{\beta\gamma} = W^{\alpha\gamma} = 0$ and $W^{\alpha\alpha} = W_{2c}^{\alpha\alpha}$, $W^{\beta\beta} = W_1^{\beta\beta}$, $W^{\gamma\gamma} = W_{2c}^{\gamma\gamma}$.

The coefficient $W^{*\beta\gamma}$ is given by

$$\begin{aligned} W^{*\beta\gamma} &= 4[\mathcal{G}(\Delta, 2\Delta + b, \Delta + c) + \mathcal{G}(\Delta, \beta, \Delta + c) \\ &\quad + \mathcal{G}(\Delta, \Delta + b, \gamma) + \mathcal{G}(\Delta, \Delta + b, 2\Delta + c)] \\ &\quad - 2[4\mathcal{G}(\Delta, \Delta + b, \Delta + c) + \mathcal{G}(\Delta, 2\Delta + b, \gamma) \\ &\quad + \mathcal{G}(\Delta, \beta, \gamma) + \mathcal{G}(\Delta, 2\Delta + b, 2\Delta + c) \\ &\quad + \mathcal{G}(\Delta, \beta, 2\Delta + c)] \end{aligned} \tag{39}$$

and from symmetry

$$W^{*\alpha\gamma}(\alpha, \beta, \gamma) = W^{*\beta\gamma}(\beta, \gamma, \alpha) \tag{40}$$

$$W^{*\alpha\beta}(\alpha, \beta, \gamma) = W^{*\beta\gamma}(\gamma, \beta, \alpha). \tag{41}$$

The coefficient $W_1{}^{\beta\beta}$ is given by

$$\begin{aligned} W_1{}^{\beta\beta} &= 4\big(2\mathcal{F}(\Delta, \Delta + b, \Delta) - \mathcal{F}(\Delta, b, \Delta) \\ &\quad - \mathcal{F}(\Delta, 2\Delta + b, \Delta)\big) \end{aligned} \tag{42}$$

and from symmetry

$$W_1{}^{\gamma\gamma}(\alpha, \beta, \gamma) = W_1{}^{\beta\beta}(\beta, \gamma, \alpha) \tag{43}$$

$$W_1{}^{\alpha\alpha}(\alpha, \beta, \gamma) = W_1{}^{\beta\beta}(\beta, \alpha, \gamma). \tag{44}$$

The coefficient $W_{2a}^{\beta\beta}$ is given by

$$\begin{aligned} W_{2a}^{\beta\beta} &= 4[\mathcal{F}(2\Delta + a, 0, \Delta) - 2\mathcal{F}(\Delta + a, 0, \Delta) \\ &\quad + \mathcal{F}(a, 0, \Delta) - \mathcal{F}(2\Delta + a, \Delta, \Delta) \\ &\quad + 2\mathcal{F}(\Delta + a, \Delta, \Delta) - \mathcal{F}(a, \Delta, \Delta)] \end{aligned} \tag{45}$$

and from symmetry

$$W_{2b}^{\beta\beta}(\alpha, \beta, \gamma) = W_{2a}^{\beta\beta}(\gamma, \beta, \alpha) \tag{46}$$

$$W_{2c}^{\alpha\alpha}(\alpha, \beta, \gamma) = W_{2a}^{\beta\beta}(\beta, \alpha, \gamma) \tag{47}$$

$$W_{2a}^{\gamma\gamma} = W_{2a}{}^{\beta\beta} \quad W_{2b}^{\alpha\alpha} = W_{2b}{}^{\beta\beta} \quad W_{2c}^{\gamma\gamma} = W_{2a}{}^{\alpha\beta}. \tag{48}$$

The coefficient $W_3{}^{\beta\beta}$ is given by

$$\begin{aligned} W_3^{\beta\beta} &= 2\big(\mathcal{F}(2\Delta + a, 0, 2\Delta + c) \\ &\quad - 2\mathcal{F}(2\Delta + a, 0, \Delta + c) + 2\mathcal{F}(\Delta + a, 0, c) \\ &\quad - 2\mathcal{F}(\Delta + a, 0, 2\Delta + c) \\ &\quad + 4\mathcal{F}(\Delta + a, 0, \Delta + c) \\ &\quad - 2\mathcal{F}(\Delta + a, 0, c) + \mathcal{F}(a, 0, 2\Delta + c) \\ &\quad - 2\mathcal{F}(a, 0, \Delta + c) + \mathcal{F}(a, 0, c)\big) \\ &\quad - 2\big(\mathcal{F}(2\Delta + a, \Delta, 2\Delta + c) \\ &\quad - 2\mathcal{F}(2\Delta + a, \Delta, \Delta + c) + \mathcal{F}(2\Delta + a, \Delta, c) \\ &\quad - 2\mathcal{F}(\Delta + a, \Delta, 2\Delta + c) \\ &\quad + 4\mathcal{F}(\Delta + a, \Delta, \Delta + c) \\ &\quad - 2\mathcal{F}(\Delta + a, \Delta, c) + \mathcal{F}(a, \Delta, 2\Delta + c) \\ &\quad - 2\mathcal{F}(a, \Delta, \Delta + c) + \mathcal{F}(a, \Delta, c)\big) \end{aligned} \tag{49}$$

and from symmetry

$$W_3^{\gamma\gamma}(\alpha, \beta, \gamma) = W_3{}^{\beta\beta}(\alpha, \gamma, \beta) \tag{50}$$

$$W_3{}^{\alpha\alpha}(\alpha, \beta, \gamma) = W_3{}^{\alpha\alpha}(\beta, \alpha, \gamma). \tag{51}$$

The coefficient $W_4^{\beta\beta}$ is given by

$$\begin{aligned} W_4^{\beta\beta} &= 2[(\mathcal{F}(2\Delta + a, \Delta + b, 2\Delta + c) \\ &\quad + \mathcal{F}(2\Delta + a, \Delta + b, \gamma) \\ &\quad + 4\mathcal{F}(\Delta + a, \Delta + b, \Delta + c) \\ &\quad + \mathcal{F}(\alpha, \Delta + b, 2\Delta + c) + \mathcal{F}(\alpha, \Delta + b, \gamma) \\ &\quad + \mathcal{F}(2\Delta + a, \beta, \Delta + c) \\ &\quad + \mathcal{F}(\Delta + a, \beta, 2\Delta + c) \\ &\quad + \mathcal{F}(\Delta + a, \beta, \gamma) + \mathcal{F}(\alpha, \beta, \Delta + c) \\ &\quad + \mathcal{F}(2\Delta + a, 2\Delta + b, \Delta + c) \\ &\quad + \mathcal{F}(\Delta + a, 2\Delta + b, 2\Delta + c) \\ &\quad + \mathcal{F}(\Delta + a, 2\Delta + b, \gamma) \\ &\quad + \mathcal{F}(\alpha, 2\Delta + b, \Delta + c)] \\ &\quad - 4[\mathcal{F}(2\Delta + a, \Delta + b, \Delta + c) \\ &\quad + \mathcal{F}(\Delta + a, \Delta + b, 2\Delta + c) \\ &\quad + \mathcal{F}(\Delta + a, \Delta + b, \gamma) + \mathcal{F}(\alpha, \Delta + b, \Delta + c)] \\ &\quad - \mathcal{F}(2\Delta + a, \beta, 2\Delta + c) - \mathcal{F}(2\Delta + a, \beta, \gamma) \\ &\quad - 4\mathcal{F}(\Delta + a, \beta, \Delta + c) + \mathcal{F}(\alpha, \beta, 2\Delta + c) \\ &\quad - \mathcal{F}(\alpha, \beta, \gamma) - \mathcal{F}(2\Delta + a, 2\Delta + b, 2\Delta + c) \\ &\quad + \mathcal{F}(2\Delta + a, 2\Delta + b, \gamma) \\ &\quad - 4\mathcal{F}(\Delta + a, 2\Delta + b, \Delta + c) \\ &\quad + \mathcal{F}(\alpha, 2\Delta + b, 2\Delta + c) \\ &\quad + \mathcal{F}(\alpha, 2\Delta + b, \gamma) \end{aligned} \tag{52}$$

and from symmetry

$$W_4^{\gamma\gamma}(\alpha, \beta, \gamma) = W_4^{\beta\beta}(\alpha, \gamma, \beta) \tag{53}$$

$$W_4^{\alpha\alpha}(\alpha, \beta, \gamma) = W_4^{\beta\beta}(\gamma, \alpha, \beta). \tag{54}$$

The coefficient $W_{5a}^{\beta\beta}$ is given by

$$
\begin{aligned}
W_{5a}^{\beta\beta} = \; & 2(\mathcal{F}(2\Delta+a,\Delta+b,\Delta) \\
& -4\mathcal{F}(\Delta+a,\Delta+b,\Delta)+2\mathcal{F}(a,\Delta+b,\Delta) \\
& -\mathcal{F}(2\Delta+a,b,\Delta)+2\mathcal{F}(\Delta+a,b,\Delta) \\
& -\mathcal{F}(a,b,c)-\mathcal{F}(2\Delta+a,2\Delta+b,\Delta) \\
& +2\mathcal{F}(\Delta+a,2\Delta+b,\Delta) \\
& -\mathcal{F}(a,2\Delta+b,c)) \qquad (55)
\end{aligned}
$$

and from symmetry

$$W_{5a}^{\alpha\alpha}(\alpha,\beta,\gamma) = W_{5a}{}^{\beta\beta}(\beta,\alpha,\gamma) \qquad (56)$$

$$W_{5b}^{\beta\beta}(\alpha,\beta,\gamma) = W_{5a}{}^{\beta\beta}(\gamma,\beta,\alpha) \qquad (57)$$

$$W_{5b}^{\gamma\gamma}(\alpha,\beta,\gamma) = W_{5a}{}^{\beta\beta}(\beta,\gamma,\alpha) \qquad (58)$$

$$W_{5c}^{\gamma\gamma}(\alpha,\beta,\gamma) = W_{5a}{}^{\beta\beta}(\alpha,\gamma,\beta) \qquad (59)$$

$$W_{5c}^{\alpha\alpha}(\alpha,\beta,\gamma) = W_{5a}{}^{\beta\beta}(\gamma,\alpha,\beta). \qquad (60)$$

References

Berkov, D. V., K. Ramstock, and A. Hubert, Solving micromagnetic problems: Towards an optimal numerical method, *Phys. Status Solidi A*, *137* (1), 207–225, 1993.

Brown, W. H., *Micromagnetics*, Krieger, Melbourne, Fla., 1978.

Chikazumi, S., and S. H. Charap, *Physics of Magnetism*, John Wiley, New York, 1964.

Dunlop, D. J., Developments in rock magnetism, *Rep. Prog. Phys.*, *53 (6)*, 707–792, 1990.

Fabian, K., A. Kirchner, W. Williams, F. Heider, A. Hubert, and T. Leibl, Three dimensional micromagnetic calculations for magnetite using fft, *Geophys. J. Int.*, *124*, 89–104, 1996.

Giles, R. C., P. R. Kotiuga, and F. B. Humphrey, 3 dimensional micromagnetic simulations on the connection machine, *J. Appl. Phys.*, *67* (9), 5821–5823, 1990.

Hillis, W. D., *The Connection Machine*, MIT Press, Cambridge, Mass., 1985.

Jackson, J. D., *Classical Electrodynamics*, p. 194, John Wiley, New York, 1975.

King, J., W. Williams, C. D. Wilkinson, S. McVite, and J. N. Chapman, Magnetic properties of magntite arrays produced by the method of electron beam lithography, *Geophys. Res. Lett.*, *23*, 2847–2850, 1996.

Kirkpatrick, S., C. D. Gelatt, and M. P. Vecci, Optimisation by simulated annealing, *Science*, *220*, 671–680, 1983.

Newell, A. J., W. Williams, and D. J. Dunlop, A generalization of the demagnetizing tensor for non-uniform magnetization, *J. Geophys. Res.*, *98* (B6), 9551–9555, 1993.

Powell, M. J. D., Restart procedures for the conjugate gradient method, *Math. Programm.*, *12*, 241–254, 1977.

Press, W. H., B. P. Flannery, S. A. Teukolsky, and W. T. Vetterling, *Numerical Recipes*, Cambridge Univ. Press, New York, 1986.

Rhodes, P., and G. Rowland, Demagnetizing energies of uniformly magnetized rectangular blocks, *Proc. Leeds Philos. Lit. Soc. Sci. Sect.*, *6*, 191–210, 1954.

Thomson, L., R. J. Enkin, and W. Williams, Simulated annealing of three-dimensional micromagnetic structures and simulated thermoremanent magnetization, *J. Geophys. Res.*, *99* (B1), 603–609, 1994.

Williams, W., and D. J. Dunlop, 3-dimensional micromagnetic modeling of ferromagnetic domain-structure, *Nature*, *337* (6208), 634–637, 1989.

Williams, W., and D. J. Dunlop, Some effects of grain shape and varying external magnetic fields on the magnetic structure of small grains of magnetite, *Phys. Earth Planet. Inter.*, *65*, 1–14, 1990.

Yuan, S. W., and H. N. Bertram, Fast adaptive algorithms for micromagnetics, *IEEE Trans. Magn.*, *28* (5), 2031–2036, 1992.

D. J. Dunlop, Department of Physics, University of Toronto, Toronto, Ontario, Canada M5S 1A7

W. Williams Department of Geology and Geophysics, University of Edinburgh, Edinburgh EH9 3JW, Scotland. (e-mail: Wyn.Williams@ed.ac.uk)

T. M. Wright, Hewlett-Packard,1400 Fountaingrove Parkway, Santa Rosa, CA 941311

(Received September 27, 1996; revised November 11, 1996; accepted November 19, 1996.)